

NOTICE: The copyright law of the United States (Title 17, U.S. Code) governs the making of photocopies or other reproductions of copyrighted material. Under certain conditions specified in the law, libraries and archives are authorized to furnish a photocopy or other reproduction. One of these specified conditions is that the photocopy or reproduction is not to be "used for any purpose other than private study, scholarship, or research."

The CDC library absorbs the cost of copyright fees charged by publishers when applicable and the cost of articles and books obtained from other libraries. Copyright fees average \$35.00 and fees charged by the lending libraries are between \$10 and \$15 per request

Biomechanical Loading of Shoulder Joints during Dynamic Cart Pushing Tasks

Yun Sun

**Keene State College
229 Main Street, Keene, NH 03435-1901**

Ashish D. Nimbarte, Majid Jaridi

**Department of Industrial and Management Systems Engineering, PO Box 6070
West Virginia University, Morgantown, WV 26506-6107**

Hongwei Hsiao

**National Institute for Occupational Safety and Health
1095 Willowdale Road, Morgantown, WV 26505**

Abstract

Manual handling of carts at workplaces are found to be associated with shoulder musculoskeletal disorders. It is currently unclear as to how the dynamic cart pushing tasks affect the musculoskeletal loading of shoulder complex joints. Therefore, the objective in this study was to evaluate dynamic pushing tasks to quantify their effects on the biomechanical loading of shoulder joints. Eight participants performed uphill cart pushing tasks on a flat, 5° and 10° ramped walkways at 20, 30, and 40 kg weight conditions. An optical motion analysis system configured with two force plates was used for data collection. The experimental data was modeled using a full-body musculoskeletal model to compute three-dimensional peak joint reaction forces acting at the sternoclavicular, acromioclavicular, and glenohumeral joints. The peak forces at the sternoclavicular joint were found to be relatively small (< 210 N) in all situations. The largest peak distraction, compression, and anterior-posterior shear forces acting at the glenohumeral joint were 1375 N, 856 N, and 619 N, respectively, during uphill pushing task on 10° ramped walkway at 40 kg weight condition. Under the same conditions, the corresponding peak forces acting at the acromioclavicular joint were 909 N, 1103 N, and 740 N, respectively.

Keywords

Dynamic pushing, biomechanical loading, modeling, shoulder joints

1. Introduction

In the United States, Musculoskeletal Disorders (MSD) impose a substantial economic burden in terms of worker compensation costs, lost wages, and decreased productivity. Conservative cost estimates vary, but a reasonable number is between \$45 and \$54 billion annually [1]. According to the Bureau of Labor Statistics [2], MSD among the occupational groups such as laborers and material movers, heavy and tractor-trailer truck drivers, and delivery service truck drivers, whose routine work demands manual material handling tasks, constitute 12 % of all MSD cases (144,910 out of 1,238,490 cases) requiring days away from work. The body parts that are most affected by manual material handling exertions include upper extremities and low back. Although upper extremities, especially shoulder MSD, are not as prominent as low back, these disorders contribute significantly to morbidity among various occupational groups and also put a substantial burden in terms of health and economics [3-7].

Among the manual material handling tasks, pushing exertions are implicated as the risk factors for the proliferation of MSD of the shoulder complex in a number of studies [8-10]. To gain insight into the causal relationship between shoulder MSD and pushing exertions, work-related pushing exertions were evaluated in a number of experimental studies. Early pushing studies focused predominantly on evaluation of static exertions [11-13]. Within industrial

settings, pushing exertions are performed under dynamic conditions and epidemiologic studies suggest that the dynamic work is associated with a higher risk of injury compared to static work[14].

Most of the recent studies focus on evaluating dynamic exertions with a primary emphasis on either investigating changes in the magnitude of hand forces corresponding to different pushing techniques [15-17] or the effect of pushing exertions on various physiological parameters, such as heart rate and oxygen uptake, etc. [18-21]. Only a few studies looked at the effect of dynamic pushing exertions on the biomechanical loading of the musculoskeletal system. Understanding of the biomechanical loading is critical in determining effective control strategies. Earlier studies employed single equivalent muscle models or quasi-static biomechanical model to estimate biomechanical loading of the low back joints during dynamic pushing exertions[22-23]. Such biomechanical models are not sensitive to the muscle co-activation that provides joint stability and controlled movement during dynamic exertions and may underestimate the mechanical loading in terms of compression and shear forces acting on the musculoskeletal system [24-27]. Recently, electromyography (EMG)-assisted optimization models, that account for the muscle co-contraction, were used by a few researchers to predict three dimensional (3D) loading during lifting and pushing exertions[25, 28]. However, these models are specific to the lumbar spine and require significant instrumentation on the worker, such as the Lumbar Motion Monitor (LMM) and several pairs of Ag/AgCl surface electrodes attached to the trunk muscles and may restrict human movement.

Thus, in spite of having a substantial epidemiological evidence relating shoulder MSD with work-related pushing exertions, effect of such exertions on the three dimensional (3D) loading of shoulder joints is not well understood. Moreover, limited research is available regarding pushing along ramps, despite high prevalence of such tasks at workplaces. Therefore, the purpose of the present study was to quantify three-dimensional (3D) musculoskeletal loading of the shoulder joints during dynamic cart pushing tasks using a comprehensive full-body musculoskeletal model. The model used in study was built with the AnyBody Modeling System ver. 4.0 [29], which is described by Damsgaard et al. [30] in detail. The musculoskeletal model is based on the public domain AnyScript Model Repository [31].

2. Methods

2.1 Approach

The effect of dynamic pushing tasks on musculoskeletal loading was examined by performing a laboratory-based study. Human participants performed cart pushing tasks on a flat and two inclined walkways under three weight conditions: 20, 30, and 40 kg. Whole body 3D joint kinematics and ground reaction force data were recorded using an eight-camera marker-based optical motion analysis system coupled with two ground reaction force platforms. The experimental data were used for running a full-body musculoskeletal model to compute the biomechanical loading of the shoulder complex joints (sternoclavicular - SC, acromioclavicular - AC, and glenohumeral - GH).

2.2 Participants

Eight young males participated in this study. The participants did not have any history of medical problems, which would have impaired their ability to perform the experimental tasks. Anyone with such a problem was excluded from the experiment. The experimental procedure was explained in detail to each participant before the experimental session, and a written consent form was read and signed by each participant. Age, weight, and height of the participants were 23.70(2.06) years, 69.79 (5.55) kg, and 1.71 (0.46) m, respectively.

2.3 Equipment

In this study, a two-wheeled Harper hand truck (CSLEDTK1935P, Harper Trucks, Inc., Wichita, KS, USA) was used. This hand truck (1.25m height \times 0.31m depth \times 0.33m width) weighs 14.3 kg and has a capacity of 317.5 kg. The height of the handle is 1.25m above ground level with the cart in an upright position and about 0.85 m in a tilted moving position. Each wheel, made of rubber, is a 0.25m pneumatic tire. In the current study, the coefficient of friction for rubber wheels on a wooden walkway was estimated to be approximately 1.3.

An eight-camera (MX-13 series) optical motion analysis system (Vicon, Nexus, UK) was used for recording the 3D kinematic data. Two Kistler force plates (type 9286, Kistler Instrument Corp., Amherst, NY, USA) embedded in the wooden walkway were used for recording the ground reaction force (GRF) data. The two force plates were mounted in the walkway with an offset of 20 cm to allow acquisition of GRF of right and left foot steps during normal gait. In

addition, this offset of 20 cm also allowed recognition of footsteps independent of force vectors exerted by the cart, which is essential for accurately running the biomechanical modeling analysis.

A hydraulic scissor lift table (EHLT-4872-3-43, Vestil Manufacturing Corp., IN, USA) was attached to one end of the wooden walkway using a hinge assembly to adjust the walkway gradients. Furthermore, four hydraulic bottle jacks (Torin Jacks, Inc., Ontario, CA) were used to support the walkway in the ramped configurations to improve its structural rigidity (Figure 1).

2.4 Experimental Design

A two-factor factorial experimental design was used. Factor 1, walkway gradient, had three fixed levels (0° , 5° and 10°). Factor 2, load weight conditions had three fixed levels (20, 30 and 40 kg). The duration of a single trial was approximately 30 seconds with a rest period of 45-60 seconds between the trials. All the trials were collected on the same day for each participant and the trial order was randomized.

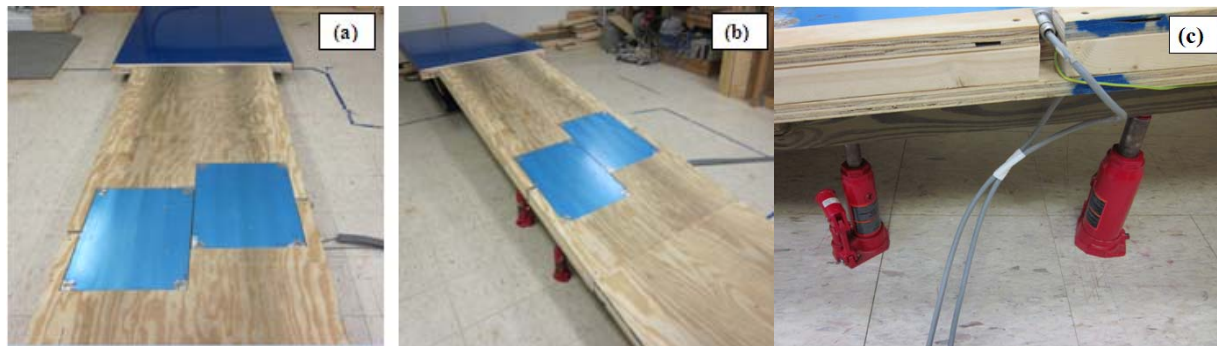


Figure 1: Experimental setup: (a) a flat walkway; (b) an inclined walkway; (c) hydraulic bottle jacks used to improve structural rigidity of walkway when inclined

2.5 Data Collection

The data collection for individual participant consists of following steps:

- 1) Each participant was briefed about the objective of the experiment.
- 2) A set of demographic and anthropometric measurements were recorded.
- 3) The participant then changed into the test shirt and pant and a set of thirty-nine reflective markers (diameter = 0.025 m) were affixed on the anatomical locations based on the Plug-in-Gait marker set. Additionally four markers were placed on the cart to track its motion during the pushing tasks.
- 4) The participants were provided with the instructions and training sessions to get them familiarized with how to perform the task.
- 5) Subsequently, participant performed the dynamic cart pushing tasks on a wooden walkway with a two-wheeled hand cart under varying levels of load weights and walkway gradients.

2.6 Data Processing and Modeling

Marker and GRF data were processed using Vicon Nexus software and exported in the C3D format. The C3D data were imported in the AnyBody modeling platform using AnyScript programming language. A full body musculoskeletal model based on the public domain AnyScript Model Repository [31] was used to model the cart pushing exertions to quantify biomechanical loading. This model consists of 750 individual muscle fascicles, 33 joints, and 34 rigid body segments. The basic model was modified by adding a cart segment in the model environment (Figure 2). This segment was defined as a rigid body, formed using eighteen nodes joined together using polyline object. Additionally, two nodes for the right and left handle were created to connect the cart with the hands. The mass properties of the cart were defined by means of a mass and an inertia tensor.

To quantify the loading of the shoulder joints during dynamic cart pushing tasks, the model was driven using the 3D marker trajectory inputs corresponding to participants' cart pushing kinematics, and GRF data recorded from the two force platforms. The data transition involved in the analysis performed in this study is graphically represented in the Figure 3. The step involved in driving a model using these data from a C3D file involves:



Figure 2: Graphical representation of the musculoskeletal model developed using AnyBody modeling system to model the cart pushing exertions

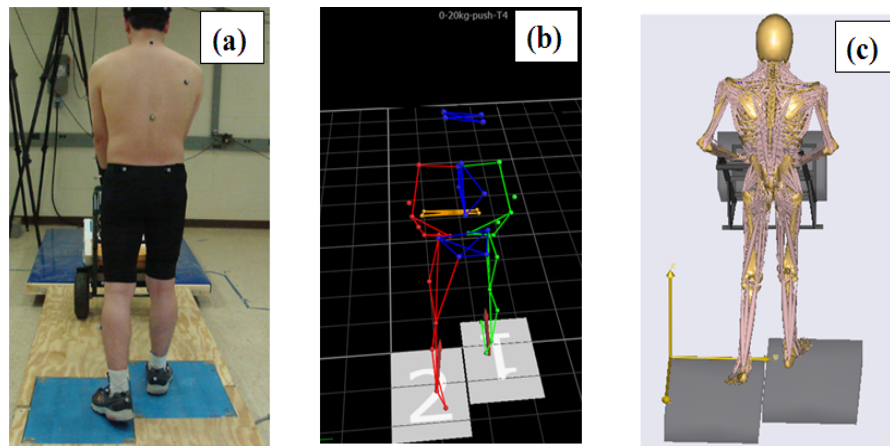


Figure 3: (a) Participant performing cart pushing task along a flat walkway; (b) Corresponding marker data labeled using Vicon Nexus software to generate the C3D file; (c) The biomechanical model developed in theAnyBody modeling systemdriven by using the C3D data

- 1) Scaling the model based on the participants' anthropometrical data
- 2) Optimizing model parameters such as marker location, segment lengths, and joint locations using 3D marker kinematics.
- 3) Performing inverse dynamics analysis to compute muscle and joint forces. In AnyBody Modeling System, the muscle force required to generate motion or sustain body posture is computed using inverse-dynamics methods by solving a multi-body dynamics problem. The muscle recruitment in the inverse dynamics process is solved using a min/max optimization procedure [32], within which the objective function is to minimize the maximal normalized muscle force. The objective function of the optimization procedure is:

$$G(f_{(m)}) = \text{Max} \left(\frac{f_{(m)i}}{F_{(m)i}} \right); i = 1, 2, \dots, N \quad (1)$$

Where, $f_{(m)}$ and $F_{(m)i}$ corresponds to the muscle force and strength at optimal length for muscle i . The objective function is constrained by the upper bound $(f_{(m)i}/F_{(m)i} \leq 1)$ and lower bound $(f_{(m)i} \geq 0)$ of force for N muscle and the following dynamic force balance equation:

$$Cf = r \quad (2)$$

Where, \mathbf{f} is a vector of muscle and joint forces; \mathbf{r} is a vector representing the external forces and inertia forces; \mathbf{C} is the coefficient matrix for the “unknown” forces in the system.

2.7 Statistical Analysis

A two factor (3×3) general linear ANOVA model was used for the statistical analysis. The independent variables were the load transferred (20 kg, 30 kg and 40 kg) and the walkway gradient (0° , 5° and 10°). The dependent variables were the 3D musculoskeletal loading of the shoulder joints. Three shoulder joints sternoclavicular (SC), acromioclavicular (AC), and glenohumeral (GH) were evaluated in terms of compression (infero-superior), and medio-lateral (ML) and anterior-posterior (AP) shear forces. Forces in the ML direction for the GH joint are termed as distraction (DIS) forces.

3. Results

3.1 Sternoclavicular Joint Loading

In general, the peak compression, and ML and AP shear forces acting at the sternoclavicular (SC) joint increased with the load weight and walkway gradient (Figure 4(a)). Overall, the magnitude of AP shear force at the SC joint was much smaller (< 60 N in all situations) compared to the peak forces in the other two directions. The interaction effect of load weight and walkway gradient was significant for the peak compression and ML shear forces acting at the SC joint (all $p < 0.01$). The results of the All-pairwise comparison test are shown in the Table 1. The effect of load weight on the mean of peak AP shear forces was more pronounced at the walkway gradient of 10° . Whereas, the mean of peak compression forces at 40 kg weight conditions was significantly higher than the 20 and 30 kg weight conditions independent of walkway gradient.

Table 1: The peak reaction forces(N) (mean (SD)) exerted during cart pushing tasks at shoulder joints in the compression or infero-superior (IS), and medio-lateral (ML) and anterior-posterior (AP) direction

Joint	Force	0°			5°			10°		
		20 kg	30 kg	40 kg	20 kg	30 kg	40 kg	20 kg	30 kg	40 kg
SC	ML	49.4 [*] (20.6) ^a	63.1 (27.2) ^a	76.2 (25.7) ^a	71.9 (16.4) ^a	72.3 (37.0) ^a	75.8 (29.8) ^a	72.7 (29.4) ^a	181.2 (42.3) ^b	200.6 (38.9) ^b
	IS	51.3 (16.7) ^a	74.4 (19.5) ^a	104.9 (28.6) ^b	71.0 (21.2) ^a	83.6 (19.0) ^a	139.5 (21.5) ^b	98.3 (25.4) ^a	147.3 (22.3) ^b	201.2 (27.5) ^c
	AP	21.7 (6.8) ^a	27.8 (10.3) ^{ab}	37.3 (7.9) ^b	26.1 (5.5) ^a	36.7 (8.2) ^{ab}	42.2 (9.2) ^b	46.5 (6.6) ^a	45.7 (11.1) ^a	58.9 (12.9) ^b
AC	ML	206.9 (38.8) ^a	305.5 (66.5) ^{ab}	412.8 (86.7) ^b	242.4 (67.1) ^a	328.1 (133.5) ^{ab}	437.2 (154.9) ^b	409.3 (156.1) ^a	549.6 (222.4) ^a	908.8 (225.6) ^b
	IS	274.6 (74.6) ^a	396.7 (95.0) ^{ab}	543.4 (132.5) ^b	306.0 (82.2) ^a	411.0 (97.0) ^a	611.6 (193.8) ^b	504.7 (144.3) ^a	773.9 (249.8) ^b	1103.2 (208.6) ^c
	AP	174.6 (56.7) ^a	232.5 (62.7) ^a	341.3 (89.9) ^b	205.7 (68.4) ^a	243.3 (77.2) ^a	356.1 (85.4) ^b	279.7 (123.8) ^a	479.1 (86.0) ^b	740.0 (106.4) ^c
GH	DIS	343.2 (96.5) ^a	488.8 (113.9) ^a	670.1 (111.9) ^b	464.9 (136.0) ^a	634.2 (167.8) ^a	841.5 (199.0) ^b	705.4 (105.8) ^a	1007.4 (159.6) ^b	1374.7 (148.8) ^c
	IS	193.0 (83.6) ^a	307.5 (136.1) ^a	476.2 (150.9) ^b	224.5 (68.6) ^a	326.4 (139.9) ^a	533.2 (228.8) ^b	447.1 (127.2) ^a	653.8 (71.1) ^b	855.9 (135.9) ^c
	AP	160.6 (42.1) ^a	254.5 (96.5) ^{ab}	320.4 (99.7) ^b	189.6 (44.5) ^a	269.4 (69.4) ^{ab}	343.0 (91.8) ^b	261.2 (52.2) ^a	461.4 (92.6) ^b	619.1 (120.2) ^c

*The alphabets (a, b, c) represent the results of All-pairwise comparison. Cells with different alphabets across same walkway gradient represent significant difference for weight conditions.

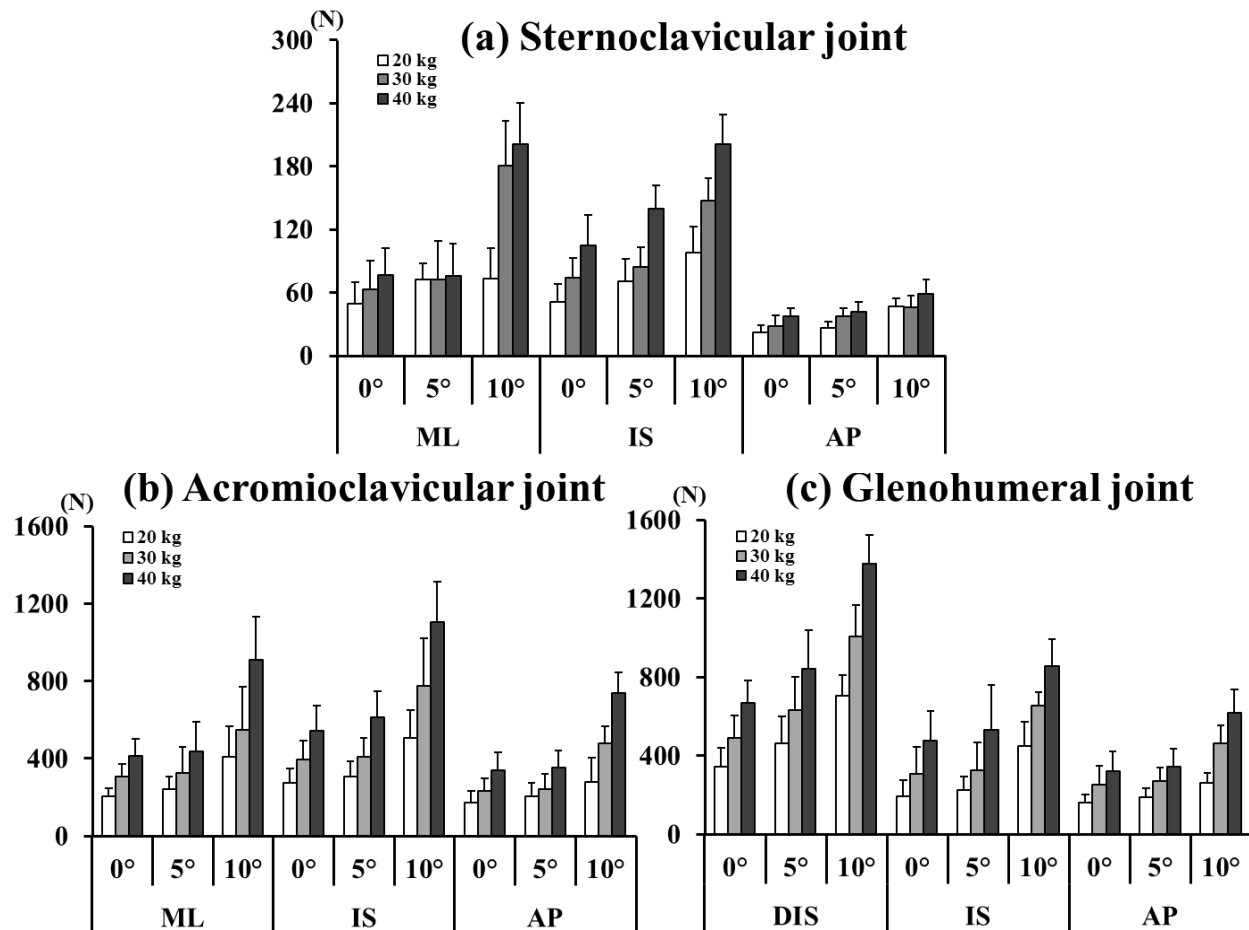


Figure 4: Loading at shoulder joints during dynamic cart pushing tasks

3.2 Acromioclavicular Joint Loading

A general trend showed that the peak forces in three directions acting at the Acromioclavicular (AC) joint increased with the increase in the load weight and walkway gradient (Figure 4(b)). Overall the magnitude of peak shear force in the AP direction was comparatively lower than the peak forces in the other two directions. Statistically, the interaction effect of the load weight and walkway gradient was significant for the peak forces in all the three directions at the AC joint (all $p < 0.01$). Independent of the walkway gradient, the mean of peak ML shear forces was significantly higher at the 40 kg weight condition than 20 kg weight condition (Table 1). The mean of peak compression and AP shear forces increased significantly with the increase in the weight from 20 to 30 to 40 kg at the walkway gradient of 10°. At walkway gradient of 0° and 5°, magnitude of these forces were significantly greater at 40 kg weight condition than 20 kg weight condition.

3.3 Glenohumeral Joint Loading

The magnitude of forces acting at the Glenohumeral (GH) joint was higher than the corresponding forces acting at the AC and SC joints. For the GH joint, among the three anatomical directions, the highest forces were exerted in the distraction direction followed by the compression and shear forces in the AP directions (Figure 4(c)). In general, the peak compression, distraction and shear forces in the AP directions at the GH joint increased corresponding to the increase in the load weight and the walkway gradient. A significant interaction effect of the load weight and walkway gradient was observed for these forces at the GH joint (all $p < 0.01$). The mean of peak forces in the all three anatomical directions increased significantly with the increase in the weight from 20 to 30 to 40 kg at the walkway gradient of 10° (Table 1). At 0° and 5° walkway gradient, magnitudes of these forces were significantly greater at 40 kg weight condition than 20 kg weight condition.

4. Discussion

In this study, 3D biomechanical loading at the sternoclavicular (SC), acromioclavicular (AC) and glenohumeral (GH) joints of the shoulder complex was estimated during dynamic cart pushing task performed under varying levels of load weight and walkway gradient. The study outcome indicate that 3D loading for the SC, AC, and GH joints was significantly affected by the weight being transfer and the gradient of the walkway. No previous study has reported the biomechanical loading of SC, AC, and GH joints in three anatomical directions during dynamic pushing exertions. A few studies have reported net moment at GH joint during pushing and pulling type of exertions [33-35] and a study of Hoozemans et al. [28] is the only available study that reported reaction forces acting at the GH joint in the inferior-superior direction. In this study, the authors have reported that the compression forces at the GH joint were significantly affected by the load weight and also presented a generalized estimating equation (GEE) for quantifying GH loading during pushing/pulling exertions. Based on this equation for the load weight of 40 kg along a horizontal surface, a compression force of 482 N was estimated at the GH joint. This value is very close to the peak compression force of 476 N estimated in the present study.

Among the three shoulder complex joints the reaction forces during the dynamic cart pushing tasks acting at the GH and AC joints were much higher than the SC joints were. This can be explained by the anatomical structure of these joints in the shoulder complex. Compared to the SC joint, the AC and GH joints require activation of higher number of muscles for stabilization during the motion. The co-contraction of the muscles around these joints contributes to the higher reaction forces at this joint. In contrast for the SC joint the range of motion is rather small and there is hardly any active muscle tissue surrounding this joint to exert forces, and consequently, forces due to muscle co-contraction are negligible [36]. A similar behavior of shoulder joints, i.e. relatively higher loading for the GH joint compared to the SC joint is also reported by van Drongelen et al. [36] during wheelchair-related propulsion activities.

The forces acting at the AC joint were found to be quite high and equivalent with the GH joint. On average the peak compression forces acting at the AC joints were 1.25 times that of GH joint. The peak of shear forces acting the AC joints were 0.6 and 1.04 times that of GH joint in the ML (or DIS) and AP directions, respectively. In the existing literature the focus has always been on the loading at the GH joint to evaluate the risk of shoulder MSD during pushing exertions. The results of this study show that, in addition to the GH joint, AC joint is also loaded to higher levels during the pushing exertions and should be considered while evaluating risks of shoulder MSD.

From the risk assessment point of view, little is known about the safe loading limits for the shoulder joints. If a tolerance limit of 500 N was considered which is same as the limits used by McGill [37] for the shear loading of low back then pushing exertions performed using load weights of 30 kg and 40 kg along a walkway gradient of 10° would cause significant loading for the AC joint in the ML direction. For the AC joint, pushing using the load weight of 40 kg along a 10° inclined walkway would also cause significant loading in the AP direction. For the GH joint, pushing exertions performed using load weight of 40 kg along a flat walkway, as well as using 30 kg and 40 kg along a walkway gradient of 5°, would cause significant loading in the distraction (lateral) direction. In addition, pushing along a walkway gradient of 10° would cause significant loading in the distraction (lateral) direction under all three weight conditions (20, 30, and 40 kg), as well as in the AP direction under 40 kg weight condition. However, these claims were based on a tolerance limit of 500 N for the shear loading. Future studies evaluating accurate tolerance limits for the shoulder joints are needed to more accurately understand the risk of injuries during occupational pushing exertions.

References

1. Dunning, K.K., et al., 2010, "Costs by industry and diagnosis among musculoskeletal claims in a state workers compensation system: 1999-2004," *American Journal of Industrial Medicine*, 53, 276-284.
2. Bureau of Labor Statistics, 2010, "Nonfatal Occupational Injuries and Illnesses Requiring Days Away From Work, 2009," [cited 2011 April 12], Available from: <http://www.bls.gov/news.release/osh2.nr0.htm>.
3. Nonnenmann, M., et al., 2008, "Musculoskeletal symptoms of the neck and upper extremities among Iowa dairy farmers," *American Journal of Industrial Medicine*, 51(6), 443-451.
4. Hess, J., et al., 2010, "Ergonomic evaluation of masons laying concrete masonry units and autoclaved aerated concrete," *Applied Ergonomics*, 41(3), 477-483.

5. Holmström, E., Lindell, J., and Moritz, U., 1992, "Low back and neck/shoulder pain in construction workers: Occupational workload and psychosocial risk factors. Part 2: relationship to neck and shoulder pain," *Spine*, 17(6), 672-677.
6. Grooten, W., et al., 2004, "Seeking care for neck/shoulder pain: A prospective study of work-related risk factors in a healthy population," *Journal of occupational and environmental medicine*, 46(2), 138-146.
7. Cassou, B., et al., 2002, "Chronic neck and shoulder pain, age, and working conditions: Longitudinal results from a large random sample in France," *Occupational and Environmental Medicine*, 59(8), 537-544.
8. van der Beek, A., et al., 1993, "Loading and unloading by lorry drivers and musculoskeletal complaints," *International Journal of Industrial Ergonomics*, 12(1-2), 13-23.
9. Smedley, J., et al., 2003, "Risk factors for incident neck and shoulder pain in hospital nurses," *Occupational and Environmental Medicine*, 60(11), 864-869.
10. Hoozemans, M., et al., 2002, "Pushing and pulling in association with low back and shoulder complaints," *Occupational and Environmental Medicine*, 59(10), 696-702.
11. Chaffin, D., Andres, R., and Garg, A., 1983, "Volitional postures during maximum push/pull exertions in the sagittal plane," *Human Factors*, 25(5), 541-550.
12. Kroemer, K., 1974, "Horizontal push and pull forces exorable when standing in working positions on various surfaces," *Applied Ergonomics*, 5, 94-102.
13. Ayoub, M., and Mcdaniel, J., 1974, "Effects of operator stance on pushing and pulling tasks," *American Institute of Industrial Engineering Transactions*, 6, 185-195.
14. Marras, W., et al., 1993, "The role of dynamic three-dimensional trunk motion in occupationally-related low back disorders: the effects of workplace factors, trunk position, and trunk motion characteristics on risk of injury," *Spine*, 18(5), 617-628.
15. Todd, A., 2005, "Current trends in research focused on pushing and pulling." in 4th International Cyberspace Conference on Ergonomics, Johannesburg.
16. Resnick, M., and Chaffin, D., 1995, "An ergonomic evaluation of handle height and load in maximal and submaximal cart pushing," *Applied Ergonomics*, 26(3), 173-178.
17. Bennett, A., et al., 2008, "The effects of load and gradient on hand force responses during dynamic pushing and pulling tasks," *Ergonomics SA: Journal of the Ergonomics Society of South Africa*, 20(1), 3-15.
18. van der Beek, A., and Frings-Dresen, M., 1995, "Physical workload of lorry drivers: a comparison of four methods of transport," *Ergonomics*, 38(7), 1508-1520.
19. van der Beek, A., et al., 2000, "Gender differences in exerted forces and physiological load during pushing and pulling of wheeled cages by postal workers," *Ergonomics*, 43(2), 269-281.
20. Frings-Dresen, M., et al., 1995, "Guidelines for energetic load in three methods of refuse collecting," *Ergonomics*, 38(10), 2056-2064.
21. Frings-Dresen, M., et al., 1995, "The daily work load of refuse collectors working with three different collecting methods: a field study," *Ergonomics*, 38(10), 2045-2055.
22. Jäger, M., et al., 2007, "Load on the lumbar spine of flight attendants during pushing and pulling trolleys aboard aircraft," *International Journal of Industrial Ergonomics*, 37(11-12), 863-876.
23. Schibye, B., et al., 2001, "Mechanical load on the low back and shoulders during pushing and pulling of two-wheeled waste containers compared with lifting and carrying of bags and bins," *Clinical Biomechanics (Bristol, Avon)*, 16(7), 549-559.
24. Garg, A., and Kapellusch, J., 2009, "Applications of biomechanics for prevention of work-related musculoskeletal disorders," *Ergonomics*, 52(1), 36-59.
25. Knapik, G., and Marras, W., 2009, "Spine loading at different lumbar levels during pushing and pulling," *Ergonomics*, 52(1), 60-70.
26. Lee, K., et al., 1989, "Lower back muscle forces in pushing and pulling," *Ergonomics* 32 (12), 1551-1563.
27. Andres, R., and Chaffin, D., 1991, "Validation of a biodynamic model of pushing and pulling," *Journal of biomechanics*, 24(11), 1033-1045.
28. Hoozemans, M., et al., 2004, "Mechanical loading of the low back and shoulders during pushing and pulling activities," *Ergonomics*, 47(1), 1-18.
29. AnyBody Technology, 2006, Available from: www.anybodytech.com.
30. Damsgaard, M., et al., 2006, "Analysis of musculoskeletal systems in the AnyBody Modeling System," *Simulation Modelling Practice and Theory*, 14(8), 1100-1111.
31. AnyBody Technology, 2011, "The AnyScript Model Repository," Available from: <http://www.anybody.aau.dk/?Repository>.

32. Rasmussen, J., Damsgaard, M., and Voigt, M., 2001, "Muscle recruitment by the min/max criterion - a comparative numerical study," *Journal of Biomechanics*, 34(3), 409-415.
33. De Looze, M., et al., 2000, "Force direction and physical load in dynamic pushing and pulling," *Ergonomics*, 43(3), 377-390.
34. Van der Woude, L., et al., 1995, "Effect of push handle height on net moments and forces on the musculoskeletal system during standardized wheelchair pushing tasks," *Prosthetics and Orthotics International*, 19(3), 188-201.
35. Abel, E., and Frank, T., 1991, "The design of attendant propelled wheelchairs," *Prosthetics and Orthotics International*, 15(1), 38.
36. van Drongelen, S., van der Woude, L., and Veeger, H., 2011, "Load on the shoulder complex during wheelchair propulsion and weight relief lifting," *Clinical Biomechanics*, 26(5), 452-457.
37. McGill, S., 2007, "Low back disorders: evidence-based prevention and rehabilitation.." Champaign, IL: Human Kinetics Publishers.